

FIRST BEAM HALO MEASUREMENTS USING WIRE SCANNERS AT THE EUROPEAN XFEL

S. Liu[†], V. Balandin, B. Beutner, W. Decking, L. Fröhlich, N. Golubeva, T. Lensch, DESY, Hamburg, Germany

Abstract

Beam halo measurements and collimations are of great importance at the European XFEL, especially for the operation at high repetition rates (27000 pulses/s). First beam halo measurements have been performed during the commissioning using the wire scanners installed before and after the ~200 m long post-linac collimation section. We present the measurement results and the comparison of beam halo distributions before and after the collimation section.

INTRODUCTION

The European XFEL [1] is driven by a ~1.7 km long superconducting linear accelerator followed by three undulator systems called SASE1, SASE2 and SASE3 with 35, 35 and 21 undulator segments (each 5 m long), respectively. It operates in bunch train mode with 10 Hz of repetition rate and a maximum number of 2700 electron bunches can be generated per macro pulse with a spacing of 220 ns. The maximum beam power can be generated is more than 500 kW. It is well known that, a common issue for high power machines is the control of beam losses, since the beam losses can cause damages to different components of the machine. In the case of European XFEL, the main concern is the damage to the undulators. Therefore, a ~200 m long post-linac collimation (CL) section is designed to collimate the beam halo and dark current before the undulator section [2].

The CL section has two arcs and one straight section in between as phase shifter. The betatron functions at the collimator locations can be varied by tuning the quadrupoles in the matching sections before and after the collimation section, and in the phase shifter. This tuning includes also the possibility of FODO-like transport through the whole collimation section. This feature brings the flexibility to operate the collimation section in different optics modes. At the beginning of the commission, the FODO-like mode is used. Recently, another two optics modes have also been tested. One is the mode A optics: the standard collimation optics with beta functions (of about 200m) at the collimator locations, and the other is the mode B optics (see Fig.1): the relaxed optics with smaller beta functions (of about 100m) at the collimator locations.

The efficiency of beam halo collimation has been studied in simulations during the design of the collimation section [2] and also for the implementation of Hard X-ray self-seeding, where a diamond crystal will be inserted close to the beam in the undulator sections [3]. For the experimental study, different instruments can be used to

measure the beam halo (e.g. YAG:Ce screen [4], diamond detector [5] and wire scanners [6]). At the European XFEL, the wire scanners (WS's) [7] installed before and after the collimation section can be used. In this paper, we present the design and commissioning of the WSs followed by the first beam halo measurements using the WSs with the collimation optics mode B.

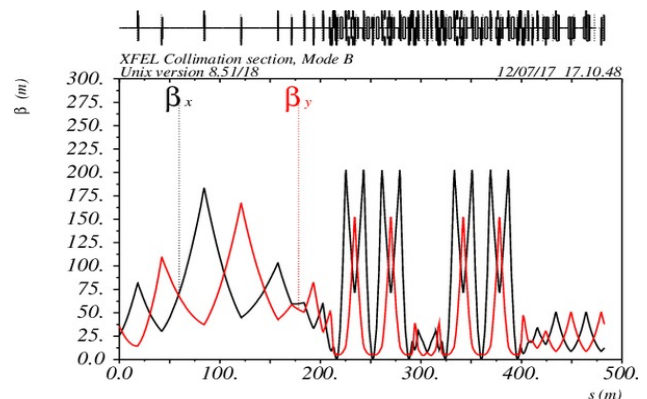


Figure 1: Betatron functions in the collimation section for optics mode B.

WIRE SCANNERS AT THE EUROPEAN XFEL

At the European XFEL, there are in total 4 sets of WSs installed in L3 (before CL), TL (after CL), T1 (before SASE2) and T4 (before SASE3), respectively. Each set of WS consists of three WS units, and each unit has one horizontal and one vertical WS stage. The WSs are installed in the optics matching sections, this allows for emittance measurement and optics matching purposes (especially at high repetition rate) in complementary to the measurements using the scintillation screens [5] (usu-

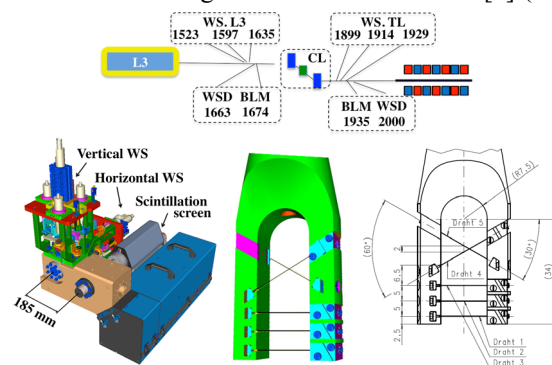


Figure 2: Two WS sets before and after CL section and their detectors (top), the number indicates their location from the gun in meters. Layout of WS stations with scintillation screen layout (bottom-left) and the wire scanner fork with tungsten wires (bottom-right).

[†] shan.liu@desy.de

Content from this work may be used under the terms of the CC BY 3.0 licence (© 2018). Any distribution of this work must maintain attribution to the author(s), title of the work, publisher, and DOI.

ally only for single bunch) installed on the same stages at around 185 mm in front of the WS (see Fig. 2).

On one WS stage, there are in total 5 tungsten wires mounted on one fork with the orientations as indicated in Fig. 2. The diameters of the first three wires are 50 μm , and 20 μm , respectively. The vacuum chamber diameter is 40.5 mm, so a well-aligned beam center should be located at around 20 mm. Since we have observed halos even at more than 10 mm away from the beam core (see Fig. 4 lower-left), and the spacing between each wire is 5 mm, so the measured signal can be biased by the background (BG) generated by the halo hitting on the other wires or even on the supporting fork itself. Therefore, in our measurements, we used only the first wire (50 μm) for the beam halo measurements.

The WSs are designed to operate in the fast scan mode with the maximum speed of 1 m/s to minimize the influence on the beam. Meanwhile, they can also be operated in slow scan mode. For the first measurements, we used only the slow scan mode.

WS detectors and the beam loss monitors

The WS detectors (WSDs) are made of plastic scintillating fibers optically coupled to photomultipliers (PMT). They are rolled on the beam pipes downstream of the WSs to detect the showers generated in the beam pipes by the scattered electrons and the bremsstrahlung photons. The locations of the detectors are chosen to maintain a good signal to noise ratio (SNR). There are two WSDs for each set of WS. In addition to the WSDs, the beam loss monitors (BLMs) [6] can also be used to detect the losses generated by the wires passing through the beam. Since the BLMs are more sensitive to low losses, they are more suitable for beam halo measurements than the WSDs¹.

Commissioning of the WSs

Beam size measurements have been performed using the WSs during the commissioning of the WSs (with 500 pC, compressed beam). The measured beam sizes have been compared with the measured beam sizes by the scintillating screens installed on the same stages (see Fig. 2 left). One example of the comparison is shown in Fig. 3. is a discrepancy in the beam size measured by the WS and the

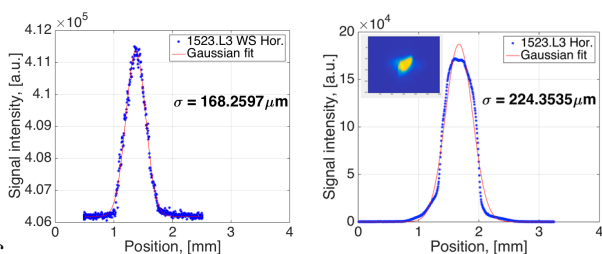


Figure 3: Horizontal beam size measured by the wire scanner (left) and the screen (right).

¹ For the beam core scan, however, the BLM signals are saturated, so only WSD signals can be used. Meanwhile, the WSD pedestal level is apparently too high to measure the beam halo.

² We assume this is due to the saturation of the scintillator, however, there might be COTR effect also.

screen. By measuring with different stages of WS and screens, we have observed an increase in discrepancy with the decrease of beam sizes. Meanwhile, we can see in Fig. 3 that the signal on the screen in the beam core region seems to be saturated², while on the WS it is well fitted to the Gaussian distribution. Therefore, we think the WS measured beam sizes are more reliable than the screen.

FIRST BEAM HALO MEASUREMENT RESULTS

First beam halo measurements have been performed with the collimation optics mode B (see Fig. 1) using one WS in front of the CL section (1523.L3) and two WSs after CL section (1899.TL and 1914.TL) (see Fig. 2, top). The beam charge is ~ 500 pC and the beam is compressed with nominal compression. During the measurements, three of the four collimators were set to 4 mm diameter aperture and the third main collimator was set to 6 mm diameter aperture.

Before scanning the beam, we registered the pedestal level of the BLMs, and scanned the dark current³. Then, the beam core is scanned and beam size is extracted from the Gaussian fit of the beam core measured by the WSD. After the beam core scan, a larger range ($> \pm 10 \sigma$) scan is performed to measure the beam halo using several downstream BLMs. The beam halo measurement results are presented in Fig. 4. Only the signal from the BLM with the highest SNR is shown. The pedestal is subtracted from the distributions.

Since the BLMs are saturated in the beam core region, we reconstructed the beam core based on the beam sizes measured by the WSD. In the reconstruction, we try to keep at least two points, which overlap with the Gaussian beam core. However, the saturation level of the BLMs is unknown⁴. Besides, there is a constant BG from the beam losses without the wire (or from the electronics), and the beam halo below this BG level cannot be detected. Therefore, when the halo is below the BG level, we can only set an upper limit on the halo level with respect to the beam core intensity.

From Fig. 4 (lower-left) we can see that before the CL section at 1523.L3, there is a rather long tail of vertical halo lasting up to -17 mm away from the beam core. This tail continues to increase on the right side (lower side) of the beam core, which indicates that the signal is strongly affected by the BG generated by other wires or the fork. This effect can also be observed in the horizontal measurement, as shown in Fig. 4 (upper-left). The visible horizontal and vertical beam halo level before the CL section at -10σ is around 10^{-3} and 10^{-2} of I_{peak} , respectively.

In Fig. 4 (middle and right) one can also see that the

³ The averaged absolute readout of the pedestal from BLM.1674.CL is $\sim 3 \times 10^{-3}$, and from BLM.1935.TL is $\sim 5 \times 10^{-3}$. During the measurements, the dark current level is below the pedestal level, therefore, we couldn't see it.

⁴ The BLMs signals are not calibrated, so the saturation level can differ from one BLM to another.

beam halo shapes measured by the two WSs after the CL section are quite similar, and the halo levels are also quite consistent. The visible horizontal and vertical beam halo level at -10σ are both below 10^{-4} of I_{peak} , and beyond 10σ the beam halo is below the pedestal level. Meanwhile, we can see that the horizontal beam halo distribution is asymmetric (more halos are measured on the left side than on the right side) and the vertical beam halo is more or less symmetric. This is maybe due to the horizontal misalignment of the beam with respect to the collimators. Besides, this also indicates that there is less beam halo left after collimation and the measurements are less (or almost not) affected by the BG generated by the other wires.

By looking at the distributions (see Fig. 4) and comparing the upper limit of halo level with respect to the I_{peak} (see Table.1), we can conclude that the halo are significantly collimated in the collimation section. The halo intensity at -10σ position decreased at least by factor 10 horizontally and factor 100 vertically after the CL section.

Table 1: Comparison of visible halo level at $-10\sigma_{x,y}$ before and after CL.

	Before CL	After CL	
	1523.L3, [I_{peak}]	1899.TL, [I_{peak}]	1914.TL, [I_{peak}]
X	$\sim 10^{-3}$	$< 10^{-4}$	$< 10^{-4}$
Y	$\sim 10^{-2}$	$< 10^{-4}$	$< 10^{-4}$

SUMMARY AND PROSPECTS

We have demonstrated the first beam halo measurements at the European XFEL with mode B collimation optics using the WSs before and after the CL section. In order to cover a large dynamic range, we have used the WSD for beam core measurement and the BLMs for

beam halo measurement. By reconstructing the beam core using the WSD measured beam size, we can set the upper limits of the beam halo levels, which allows us to compare the beam halo level before and after the CL section. According to the comparison, we can conclude that the beam halo is significantly collimated by the collimators. The first measurements show that the horizontal and vertical beam halo are at least factor 10 and 100 less at -10σ after the CL section.

There are several ways to improve the precision and dynamic range of the measurement. Firstly, according to the first measurement results, the position of the WSD and the BLMs can be optimized to enlarge the SNR. Secondly, the WSD pedestal level can be lowered down to enable halo measurement using the WSD by changing the HV on the PMT. Last but not the least, the WS hardware can also be improved. To minimize the BG from other wires, one can kick the beam close to the edge of the vacuum chamber, where the first wire enters. However, it is better to have a single wire system for beam halo measurements. With these improvements, more detailed beam halo collimation study can be carried out to compare different collimation schemes with the simulations. The measured beam halo distributions can be used in the tracking simulations for future implementations with tight aperture requirements (e.g. HXRSS and corrugated structure).

ACKNOWLEDGEMENTS

The authors would like to thank the DESY colleagues: D. Nölle, T. Wamsat, M. Scholz for their help in experiment planning and data taking; O. Hensler for software development; A. Delfs, M. Pelzer, A. Ziegler, V. Gharibyan, H. Tiessen, I. Krouptchenkov for WS design and installation. Thanks to P. Krejcik (SLAC) for helpful discussion.

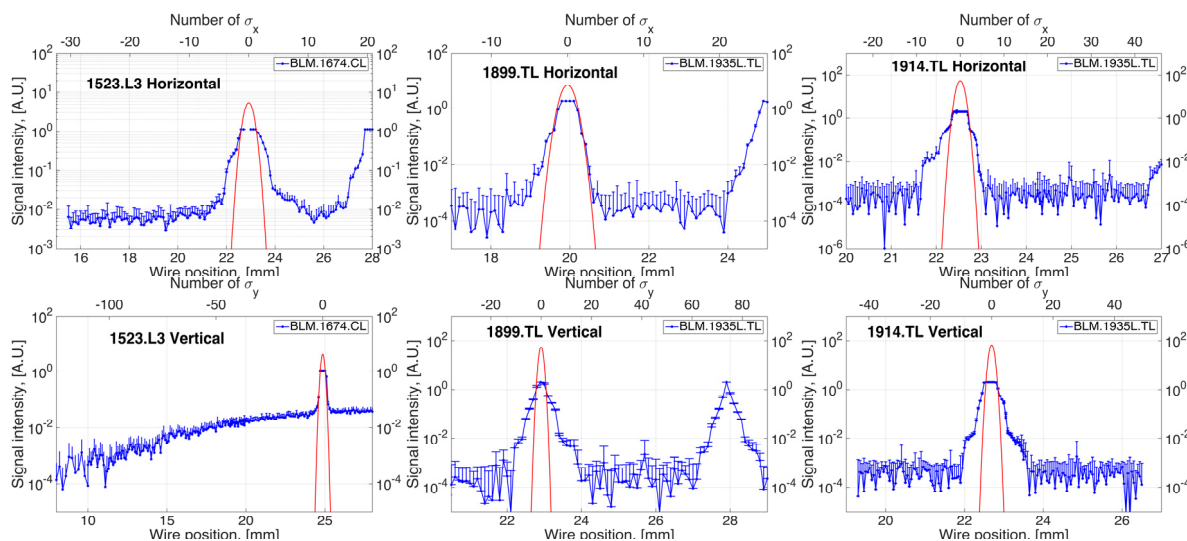


Figure 4: Horizontal (upper) and vertical (lower) beam halo measured using the WSs located before CL at 1523.L3 (left), and after CL at 1899.TL (middle) and 1914.TL (right). The blue line shows the measured distribution by the BLMs (only upper error bar is shown in log scale) and the red line shows the reconstructed Gaussian beam core.

REFERENCES

- [1] M. Altarelli, R. Brinkmann *et al.*, “XFEL: The European X-Ray Free-Electron Laser Technical Design Report”, DESY, Hamburg, Germany, DESY 2006-097, 2006.
- [2] V. Balandin, R. Brinkmann, W. Decking, and N. Golubeva, “Optics Solution for the XFEL Post-Linac Collimation Section”, DESY, Hamburg, Germany, TESLA-FEL Report 2007-05, 2007.
- [3] S. Liu, W. Decking and L. Fröhlich, “Beam Loss Simulations for the Implementation of the Hard X-Ray Self-Seeding System at European XFEL”, in *Proc. 8th Int. Particle Accelerator Conf. (IPAC'17)*, Copenhagen, Denmark, May 2017, paper WEPAB020, pp. 2611-2614.
- [4] N. Takashi, and T. Mitsuhashi, “Beam halo measurement utilizing YAG: Ce screen”, in *Proc. of 4th International Beam Instrumentation Conference IBIC'15*, Melbourne, Australia, Sept. 2015, paper TUPB024, pp.373-376.
- [5] S. Liu *et al.*, “In vacuum diamond sensor scanner for beam halo measurements in the beam line at the KEK Accelerator Test Facility”, *Nucl. Instr. Meth. A*, vol. 832, pp. 231-242, 2016.
- [6] S. Liu *et al.*, “Measurements of beam halo transverse distribution using wire scanners at ATF2” Rep. ATF-14-01, 2014.
- [7] T. Lensch *et al.*, “Wire Scanner Installation into the MicroTCA Environment for the European XFEL”, in *Proc. of IBIC'14*, Monterey, USA, Sept. 2014, paper MOPF13, pp. 73-76.
- [8] C. Wiebers *et al.*, “Scintillating screen monitors for transverse electron beam profile diagnostics at the European XFEL”, in *Proc. of IBIC2013*, Oxford, UK, Sept. 2013, paper WEPF03, pp. 807-810.
- [9] A. Kaukher *et al.*, “XFEL Beam Loss Monitor System”, in *Proc. of BIW 2012*, Virginia, USA, April 2012, paper MOPG007, pp. 35-37.